

528 **A Task Details**

529 **Setup.** Our simulation experiments are conducted on Robot Learning Benchmark (RLBench) envi-  
 530 ronment [32].

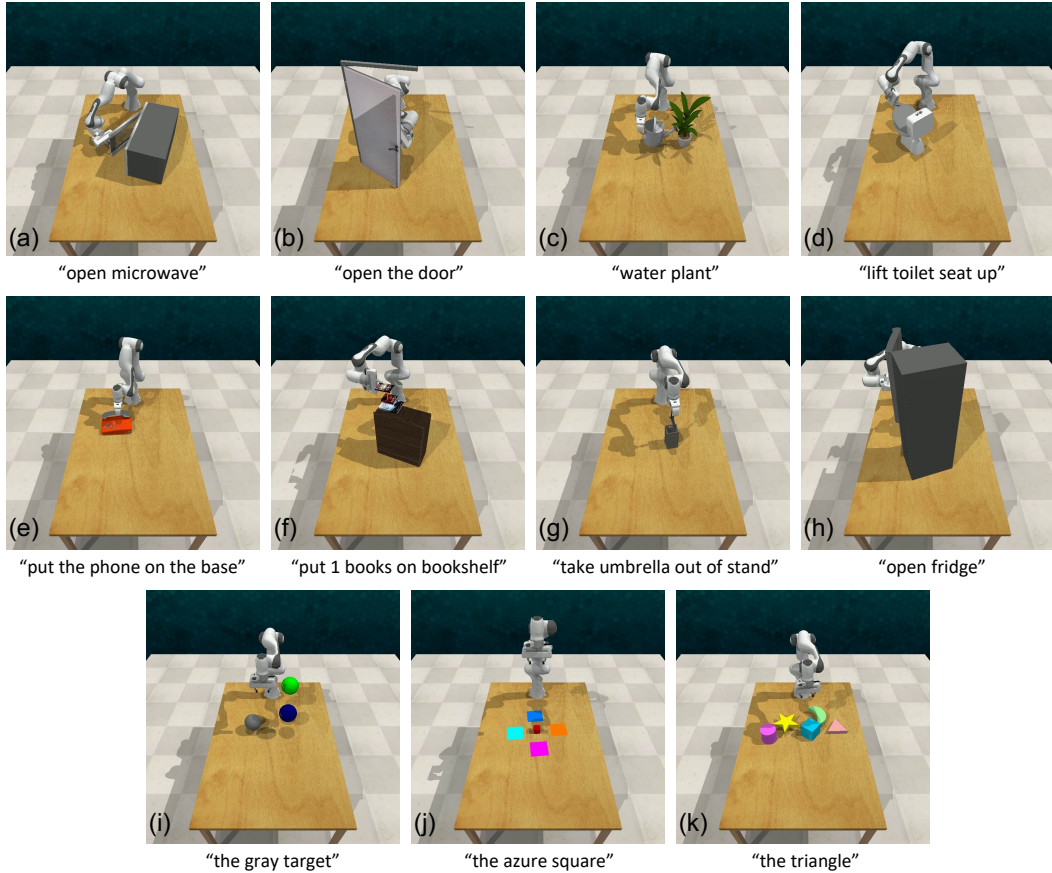


Figure 5: **RLBench Tasks.** Our simulation experiments encompass 11 tasks from RLBench. Tasks (a)-(h) serve as the basis for single-task and multi-task learning, while tasks (i)-(k) are employed to evaluate generalization performance.

531 For single-task and multi-task learning, we use 8 tasks that closely mirror real-world scenarios, for  
 532 example, our tasks incorporate objects like microwaves, plants, phones, books, and toilets that align  
 533 more closely with the reality of domestic robot environments. Our aim is to leverage the powerful  
 534 semantic understanding and spatial reasoning capabilities of SGR to facilitate the manipulation of a  
 535 diverse and complex array of objects in real-world situations.

536 For the generalization part, we conduct experiments on 3 tasks characterized by a substantial amount  
 537 of visual variations. Among the 3 tasks, two focus on color generalization, while the remaining one  
 538 is centered around shape generalization. The color variations include 20 instances:  $\text{colors} = \{\text{red, maroon, lime, green, blue, navy, yellow, cyan, magenta, silver, gray, orange, olive, purple, teal, azure, violet, rose, black, white}\}$ . The shape variations include 5 instances:  $\text{shapes} = \{\text{cube, cylinder, triangle, star, moon}\}$ .

542 As depicted in Figure 5, we utilize a diverse set of simulation tasks. In the following sections, we will  
 543 provide a detailed examination of each task, and for those tasks that have been modified compared  
 544 with the original RLBench implementation<sup>2</sup>, we will discuss the specifics of the modifications in  
 545 detail.

<sup>2</sup><https://github.com/stepjam/RLBench>

546 **A.1 Open Microwave**

547 **Filename:** open\_microwave.py

548 **Task:** Open the microwave on the table.

549 **Modified:** No.

550 **Objects:** 1 microwave.

551 **A.2 Open Door**

552 **Filename:** open\_door.py

553 **Task:** Grip the handle and push the door open.

554 **Modified:** No.

555 **Objects:** 1 door.

556 **A.3 Water Plants**

557 **Filename:** water\_plants.py

558 **Task:** Pick up the watering can by its handle and water the plant.

559 **Modified:** No.

560 **Objects:** 1 watering can and 1 plant.

561 **A.4 Toilet Seat Up**

562 **Filename:** toilet\_seat\_up.py

563 **Task:** Grip the edge of the toilet seat and lift it up to an upright position.

564 **Modified:** No.

565 **Objects:** 1 toilet with lid closed.

566 **A.5 Phone on Base**

567 **Filename:** phone\_on\_base.py

568 **Task:** Grasp the phone and put it on the base.

569 **Modified:** No.

570 **Objects:** 1 phone and 1 phone base.

571 **A.6 Put Books**

572 **Filename:** put\_books\_on\_bookshelf.py

573 **Task:** Pick up a book and place them on the top shelf.

574 **Modified:** No. The original task has 3 variations, here we only use the first variation.

575 **Objects:** 1 bookshelf and 3 books.

576 **A.7 Take out Umbrella**

577 **Filename:** take\_umbrella\_out\_of\_umbrella\_stand.py

578 **Task:** Grasp the umbrella by its handle, lift it up and out of the stand.

579 **Modified:** No.

580 **Objects:** 1 umbrella and 1 umbrella stand.

## 581 **A.8 Open Fridge**

582 **Filename:** open\_fridge.py

583 **Task:** Grip the handle and slide the fridge door open.

584 **Modified:** No.

585 **Objects:** 1 fridge with door closed.

## 586 **A.9 Reach Target**

587 **Filename:** reach\_target.py

588 **Task:** Reach the language-instructed colored ball. There are 3 balls, distinguishable solely by their  
589 colors, which are randomly distributed in space. The 3 colors are sampled from the full set of 20  
590 color instances, thus offering 20 variations based on the target color.

591 **Modified:** Yes. The sizes of the balls are enlarged so that they are distinguishable in the RGB-D  
592 input.

593 **Objects:** 3 balls.

## 594 **A.10 Slide Block**

595 **Filename:** slide\_block\_to\_color\_target.py

596 **Task:** Slide the block to the language-instructed colored square targets. There are 3 distractor target  
597 of different colors. The 4 targets are placed symmetrically and the colors are sampled from the full  
598 set of 20 color instances, which makes the 20 variations.

599 **Modified:** Yes. The original slide\_block\_to\_target.py task contains only one target. Three  
600 other targets are added.

601 **Objects:** 1 block and 4 colored target squares.

## 602 **A.11 Reach Shape**

603 **Filename:** reach\_shape.py

604 **Task:** Reach the language-instructed shape of the block. There are always 1 target shape and 4  
605 distractor shapes, which are from the 5 shape instances and randomly placed on the table. The 5  
606 different target shapes make the 5 variations.

607 **Modified:** Yes, newly added task.

608 **Objects:** 5 shapes.

# 609 **B SGR Details**

## 610 **B.1 Architecture Details**

611 **Input Data.** The SGR model takes as input RGB images  $\{I_i\}_{i=1}^K$  of size  $H \times W$  and corresponding  
612 depth images of the same size from multiple camera views. Then point cloud, represented in the  
613 robot's base frame, is derived from depth images with known camera extrinsics and intrinsics. A  
614 key detail here is that the RGB images and the organised point cloud are aligned, ensuring a one-  
615 to-one correspondence between the points across the two data forms. In the simulation setting, we  
616 have  $H = W = 128$  and  $K = 4$ , corresponding to four camera positions: front, left shoulder, right

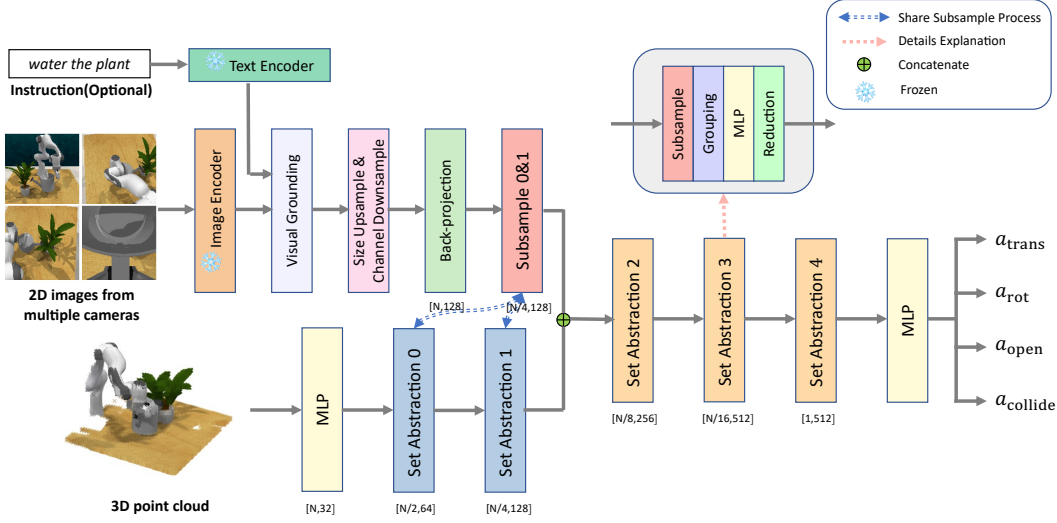


Figure 6: Architecture Details.

617 shoulder, and wrist. For real robot experiments, the setup is  $H = W = 256$  and  $K = 1$ , denoting a  
 618 single front-facing camera.

619 The model also receives proprioceptive data  $z$ , comprising four scalar values: gripper open state,  
 620 left finger joint position, right finger joint position, and action sequence timestep. Additionally, if a  
 621 task comes with language instruction  $S$ , this also forms part of the model’s input.

622 **Visual Grounding Module.** The fundamental role of a visual grounding module is to localize  
 623 visual areas that correspond to objects possessing a property as dictated by language. To equip  
 624 our manipulation model with a deep comprehension of a variety of object properties and spatial  
 625 relationships, including those not previously seen in the manipulation demonstration data, we take  
 626 inspiration from MaskCLIP [69] and PROGRAMPORT [70].

627 It’s worth noting that vanilla CLIP-ResNet-50 employs attention pooling to merge visual features  
 628 from various spatial locations into one feature vector, and then uses a linear layer  $\mathcal{F}$  as follows:

$$f_{\text{global}} = \mathcal{F} \left( \sum_i \text{softmax} \left( \frac{\text{Emb}_q(\text{AvgPool}(X)) \cdot \text{Emb}_k(X_i)^T}{C} \right) \text{Emb}_v(X_i) \right) \quad (2)$$

629 where  $X_i$  is the input feature at spatial location  $i$ ,  $\text{Emb}_{q,k,v}(\cdot)$  are linear embedding layers and  $C$  is  
 630 some fixed scalar.

631 Following MaskCLIP [69] and PROGRAMPORT [70], we establish two  $1 \times 1$  convolution layers,  
 632  $\mathcal{C}_v$  and  $\mathcal{C}_l$ , which are initialized with the weights derived from  $\text{Emb}_v$  and  $\mathcal{F}$  respectively. Applying  
 633 these layers in sequence enables the visual feature to be projected into the same space as the language  
 634 feature. Ultimately, our grounding module formulates a dense mask encompassing image segments  
 635 corresponding to the language  $S$  in the following manner:

$$f_{\text{align}} = \sum (\text{TILE}(\mathcal{H}(S)) \odot \mathcal{C}_l(\mathcal{C}_v(X))) \in \mathbb{R}^{H' \times W' \times 1} \quad (3)$$

636 where  $\mathcal{H}(S) \in \mathbb{R}^D$ ,  $\mathcal{C}_l(\mathcal{C}_v(X)) \in \mathbb{R}^{H' \times W' \times D}$  ( $H'$ ,  $W'$ ,  $D$  represent the height, width, and dimen-  
 637 sion of the pre-aligned feature respectively).  $\mathcal{H}$  is the CLIP language encoder and TILE serves  
 638 as a spatial broadcast operator that expands the language embedding vector to match the spatial di-  
 639 mensions of the visual features. The symbol  $\odot$  indicates an element-wise multiplication, while the  
 640 summation is performed over the feature dimension  $D$ . Additionally, we concatenate this feature  
 641 with the pre-aligned image feature to generate our aligned feature maps:

$$M = \text{Concat}(f_{\text{align}}, \mathcal{C}_l(\mathcal{C}_v(X))) \in \mathbb{R}^{H' \times W' \times (1+D)} \quad (4)$$

642 **Other Details.** For the image encoder, we employ CLIP-ResNet-50. To maintain consistency with  
 643 the resolution predominantly used in the pre-training of vision models, we upsample the input image  
 644 size from  $128 \times 128$  to  $256 \times 256$  in simulation experiments. The CLIP text feature exhibits a  
 645 dimensionality of 1024, and the CLIP image encoder generates a feature map of  $8 \times 8$  with 2048  
 646 channels. For the 3D encoder, we utilize PointNeXt-S. Detailed information regarding the number  
 647 of channels and sub-points in each layer of the PointNeXt network can be seen in Figure 6.

## 648 B.2 Training Details

649 **Data Augmentation.** To further improve the performance and robustness of our model, we incorpo-  
 650 rate a variety of data augmentation techniques. (1) **Translation perturbations:** during training, the  
 651 translation is perturbed with  $\pm 0.125$  m. We also experimented with rotation perturbations but found  
 652 they did not contribute to performance improvement. (2) **Color drop** is to randomly replace colors  
 653 with zero values. This technique serves as a powerful augmentation for PointNeXt, leading to sig-  
 654 nificant enhancements in the performance of tasks where color information is available. Qian et al.  
 655 [29] suggest that by implementing color drop, the network is encouraged to pay more attention to the  
 656 geometric relationships between points, leading to a boost in overall performance. (3) **Point resam-  
 657 pling** is a common technique utilized in the processing of point cloud data, often applied to adjust  
 658 the density of the point cloud. The technique involves selecting a subset of points from the original  
 659 data, thereby creating a new dataset with altered density. In our simulation experiment, we resample  
 660 4096 points from the original point cloud. (4) **Keyframe discovery and demo augmentation** [50]  
 661 [33] are to convert every data point within a demonstration into a task that involves predicting the  
 662 subsequent next-best keyframe action. Keyframes are extracted by a heuristic method: an action is  
 663 a keyframe if the joint velocities are close to zero and the gripper open state is unchanged. This  
 664 keyframe discovery strategy bypasses the need to predict long sequences of noisy actions, making  
 665 policy learning more efficient.

666 **Hyperparameters.** The configuration of hyperparameters applied in our studies can be found in  
 667 Table 3. The single-task learning and generalization experiments are trained on a single NVIDIA  
 668 GeForce RTX 3090 GPU, while the multi-task learning is trained on 8 GPUs. Since color plays  
 669 a crucial role in some tasks and disregarding color information would render these tasks unsolv-  
 670 able, such as `reach target` and `slide block`, the color drop is not utilized in the generalization  
 671 experiments.

Table 3: Hyper-parameters used in our simulation experiments.

Config	Single-task	Multi-task	Generalization
Training iterations	40,000	40,000	40,000
Lerning rate	0.0003	0.001	0.0003
Batch size	32	256	32
Optimizer	AdamW	AdamW	AdamW
Weight decay	$1 \times 10^{-6}$	$1 \times 10^{-6}$	$1 \times 10^{-6}$
Color drop	0.2	0.4	0
Instruction provided	No	Yes	Yes
Number of input points	4096	4096	4096

## 672 C Evaluation Workflow

673 **Simulation.** In pursuit of the reliability and stability of our results, our evaluation follows such sub-  
 674 sequent steps. (1) Train the agent on the train set for 40,000 training iterations and save checkpoints  
 675 every 1,000 iterations. (2) Evaluate the last 20 checkpoints for 25 episodes. (3) Evaluate the best 3  
 676 checkpoints for 100 episodes, and use the average performance of the 3 checkpoints as the results.  
 677 (4) Repeat the above steps for 3 random seeds.

Method	open microwave	open door	water plants	toilet seat up	phone on base	put books	take out umbrella	open fridge	Average
R3M	7.0 ± 5.9	24.2 ± 10.9	1.2 ± 0.7	59.7 ± 21.7	0.0 ± 0.0	15.3 ± 16.5	28.3 ± 19.0	4.7 ± 3.8	17.6
CLIP	9.1 ± 10.8	68.4 ± 8.8	4.1 ± 1.8	40.1 ± 20.8	7.3 ± 2.5	38.0 ± 16.3	66.7 ± 8.2	7.4 ± 2.8	30.2
PointNeXt <sub>TULIP</sub>	9.4 ± 1.6	60.0 ± 5.5	10.4 ± 1.6	63.0 ± 7.9	35.6 ± 4.8	41.8 ± 1.7	49.8 ± 4.2	15.3 ± 1.2	35.7
PointNeXt <sub>LIS</sub>	17.0 ± 5.4	63.8 ± 6.2	28.2 ± 2.2	52.7 ± 14.5	65.9 ± 19.9	53.1 ± 16.0	<b>95.1 ± 3.0</b>	7.3 ± 4.7	47.9
PERACT	26.9 ± 4.3	47.8 ± 41.1	<b>41.7 ± 3.1</b>	67.1 ± 4.2	0.0 ± 0.0	63.7 ± 3.5	94.4 ± 1.3	10.1 ± 3.9	44.0
<b>SGR (Ours)</b>	<b>52.6 ± 5.1</b>	<b>80.2 ± 2.7</b>	40.2 ± 8.3	<b>80.1 ± 1.2</b>	<b>81.1 ± 5.7</b>	<b>84.8 ± 7.4</b>	94.7 ± 2.3	<b>34.8 ± 2.0</b>	<b>68.6</b>

Table 4: Single-task results with mean and standard deviation (%).

Method	open microwave	open door	water plants	toilet seat up	phone on base	put books	take out umbrella	open fridge	Average
CLIP	6.0 ± 6.9	78.0 ± 2.0	6.7 ± 6.1	7.3 ± 8.1	10.0 ± 10.4	38.0 ± 21.2	15.3 ± 13.3	9.3 ± 5.0	21.3
PointNeXt <sub>LIS</sub>	22.7 ± 1.2	80.0 ± 11.1	19.3 ± 3.1	32.0 ± 20.0	69.3 ± 12.2	65.3 ± 13.3	72.0 ± 10.0	18.0 ± 2.0	47.3
PERACT	22.7 ± 2.3	58.7 ± 11.4	8.0 ± 10.6	64.7 ± 12.9	0.0 ± 0.0	47.3 ± 18.1	<b>96.0 ± 2.0</b>	4.0 ± 3.5	37.7
<b>SGR (Ours)</b>	<b>38.7 ± 15.0</b>	<b>84.0 ± 3.5</b>	<b>20.7 ± 1.2</b>	<b>67.3 ± 10.3</b>	<b>86.0 ± 10.6</b>	<b>80.0 ± 15.6</b>	88.0 ± 6.9	<b>26.7 ± 11.7</b>	<b>61.4</b>

Table 5: Multi-task results with mean and standard deviation (%).

Method	reach target		slide block		reach shape	
	Seen	Unseen	Seen	Unseen	Seen	Unseen
R3M	20.2 ± 6.2	5.5 ± 0.9	11.0 ± 5.9	3.0 ± 2.8	78.1 ± 24.5	6.7 ± 8.2
CLIP	42.0 ± 27.0	17.7 ± 4.8	49.0 ± 14.3	16.3 ± 2.8	95.5 ± 2.8	0.2 ± 0.3
PointNeXt <sub>TULIP</sub>	-	-	-	-	45.9 ± 2.0	6.7 ± 4.7
PointNeXt <sub>LIS</sub>	99.7 ± 0.3	4.0 ± 2.3	96.5 ± 1.0	6.2 ± 0.8	99.8 ± 0.4	1.8 ± 1.6
DenseFusion	71.8 ± 4.0	9.5 ± 3.1	26.5 ± 1.0	16.5 ± 1.5	99.3 ± 0.6	3.8 ± 3.4
<b>SGR (Ours)</b>	94.0 ± 2.6	<b>36.8 ± 1.6</b>	97.7 ± 1.3	<b>43.0 ± 3.0</b>	99.9 ± 0.2	<b>27.7 ± 4.0</b>

Table 6: Generalization results with mean and standard deviation (%).

678 **Real-Robot.** For the real-robot experiments, we train the agent for 40,000 iterations and simply  
679 choose the last checkpoint for evaluation, since it’s expensive to evaluate more checkpoints in the  
680 real robot. We evaluate 10 episodes per task. During the evaluation of a trained agent, the agent  
681 keeps acting until achieving the goal or reaching the maximum episode length.

## 682 D Real-Robot Setup

683 For our real-robot experiments, we use a Franka Emika Panda manipulator equipped with a parallel  
684 gripper. Perception is achieved through an Intel RealSense D415 camera, positioned in front of the  
685 scene. The camera generates RGB-D images with a resolution of  $1280 \times 720$ . We leverage the  
686 `realsense-ros`<sup>3</sup> to align depth images with color images. The extrinsic calibration between the  
687 camera frame and robot base frame is carried out using the `easy_handeye` package<sup>4</sup>.

688 When preprocessing the RGB-D images, we initially crop the  $1280 \times 720$  images to a  $720 \times 720$   
689 frame, and then resize them to  $256 \times 256$  using nearest-neighbor interpolation. This interpolation is  
690 preferred over others, such as bilinear interpolation, as the latter can cause non-existent points in the  
691 depth map, leading to a noisy point cloud. Following these steps, we can process RGB-D images in  
692 the same manner as in our simulation experiments. It’s important to note that the camera’s intrinsics  
693 must be adjusted accordingly after the images are cropped and resized. We train SGR for 40,000  
694 training steps with 64 demonstrations in total and use the final checkpoint for inference.

## 695 E Additional Results

696 For all simulation experiments, we use 3 random seeds to ensure the reliability of our results. While  
697 we present averaged results in the main body of the paper for clarity, we provide more comprehen-  
698 sive results in this section. Here, we report both the mean and standard deviation derived from our

<sup>3</sup><https://github.com/IntelRealSense/realsense-ros>

<sup>4</sup>[https://github.com/IFL-CAMP/easy\\_handeye](https://github.com/IFL-CAMP/easy_handeye)

699 simulation results to offer a complete view of our experimental outcomes. Table 4, Table 5, and Ta-  
700 ble 6 show the results of single-task learning, multi-task learning, and generalization, respectively.